Europe PMC Funders Group
Author Manuscript
Endocrinology. Author manuscript; available in PMC 2014 April 07.

Published in final edited form as:
Endocrinology. 2011 January ; 152(1): 236–246. doi:10.1210/en.2010-0925.

11β-hydroxysteroid dehydrogenase type 2 deficiency accelerates atherogenesis and causes pro-inflammatory changes in the endothelium in *Apoe*$^{-/-}$ mice

Graeme A Deuchar, PhD[#], **Danielle McLean, PhD**[#], **Patrick W.F. Hadoke, PhD**, **David G Brownstein, PhD**, **David J Webb, MD, DSci**, **John J Mullins, PhD**, **Karen Chapman, PhD**, **Jonathan R Seckl, MD, PhD**, and **Yuri V Kotelevtsev, PhD**
Centre for Cardiovascular Science, The Queen's Medical Research Institute, College of Medicine and Veterinary Medicine, University of Edinburgh, 47 Little France Crescent, Edinburgh, EH16 4TJ, UK

[#] These authors contributed equally to this work.

Abstract

Mineralocorticoid receptor (MR) activation is pro inflammatory and pro atherogenic. Antagonism of MR improves survival in humans with congestive heart failure caused by atherosclerotic disease. In animal models, activation of MR exacerbates atherosclerosis. The enzyme 11β-hydroxysteroid dehydrogenase 2 (11β-HSD2) prevents inappropriate activation of the mineralocorticoid receptor (MR) from inappropriate activation by glucocorticoids by inactivating glucocorticoids in mineralocorticoid-target tissues. To determine whether glucocorticoid-mediated activation of MR increases atheromatous plaque formation we generated *Apoe*$^{-/-}$*/11β-HSD2*$^{-/-}$ double-knockout (E/b2) mice. On chow diet, E/b2 mice developed atherosclerotic lesions by 3 months of age, while *Apoe*$^{-/-}$ mice remained lesion-free. Brachiocephalic plaques in 3 month-old E/b2 mice showed increased macrophage and lipid content and reduced collagen content compared to similar sized brachiocephalic plaques in 6 month old *Apoe*$^{-/-}$ mice. Crucially, treatment of E/b2 mice with eplerenone, an MR antagonist, reduced plaque development and macrophage infiltration while increasing collagen and smooth muscle cell content without any effect on systolic blood pressure (SBP). In contrast, reduction of SBP in E/b2 mice using the epithelial sodium channel (ENaC) blocker amiloride produced a less profound atheroprotective effect. Vascular cell adhesion molecule 1 (VCAM-1) expression was increased in the endothelium of E/b2 mice compared to *Apoe*$^{-/-}$ mice. Similarly, aldosterone increased VCAM-1 expression in mouse aortic endothelial cells, an effect mimicked by corticosterone only in the presence of an 11β-HSD2 inhibitor. Thus, loss of 11β-HSD2 leads to striking atherogenesis associated with activation of MR stimulating pro-inflammatory processes in the endothelium of E/b2 mice.

Keywords

atherosclerosis; mineralocorticoid receptor; 11β-hydroxysteroid dehydrogenase

Atherosclerosis is a chronic inflammatory response to injury in the vessel wall, yet the initiating events that precede leukocyte accumulation and fat deposition leading to plaque development remain poorly defined. Mineralocorticoid receptor (MR) antagonists,

Correspondence to Yuri Kotelevtsev, PhD, Centre for Cardiovascular Science, The Queen's Medical Research Institute, 47 Little France Crescent, Edinburgh, EH16 4TJ, UK. Tel: +44-131-242-9212, Fax: +44 870 1342778 ykotelev@staffmail.ed.ac.uk.

Disclosure Summary: The authors have nothing to disclose.

Europe PMC Funders Author Manuscripts
Europe PMC Funders Author Manuscripts

Europe PMC Funders Author Manuscripts

Europe PMC Funders Author Manuscripts

administered as diuretics at doses that do not significantly lower blood pressure, improve survival in heart failure (1) and acute myocardial infarction (2) in humans. Activation of MR in the vasculature is also pro-inflammatory and pro-atherogenic (3) suggesting protective effects of MR antagonism on the cardiovascular system, independent of blood pressure. However, the mechanisms asociated with these cardio-protective effects in humans are yet to be determined. MR are also high affinity glucocorticoid receptors (4), yet in mineralocorticoid target tissues, including the distal nephron, MR are selective for aldosterone, their physiological ligand, despite higher (~100-fold) circulating levels of glucocorticoid (5). This selectivity at least in part is a consequence of pre-receptor metabolism of glucocorticoids to intrinsically inert 11-keto-glucocorticoids by 11β-hydroxysteroid dehydrogenase type 2 (11β-HSD2) (6). The pathophysiologic importance of 11β-HSD2 is demonstrated in patients with the syndrome of apparent mineralocorticoid excess (SAME) caused by mutations in HSD11B2, the human gene encoding 11β-HSD2(7). Loss of 11β-HSD2 results in inappropriate activation of MR by glucocorticoids in the distal nephron causing hypokalemia and hypertension(8). Similarly, *11β-HSD2* $^{-/-}$ mice are also hypertensive, with activation of MR in the distal nephron causing increased sodium re-absorption and potassium excretion (9).

Evidence supports a pro-atherogenic action of cortisol within the vessel wall (10). Glucocorticoid pharmacotherapy in humans is associated with increased cardiovascular events (11).

We and others have demonstrated the existence of the MR/11β-HSD2 system in nonepithelial tissues, including the vasculature (12). Thus, pro-atherogenic effects of MR activation could be mediated directly by increased mineralocorticoid hormones or through bypass or reduced activity of vascular 11β-HSD2, permitting glucocorticoid activation of vascular MR. All known inhibitors of 11β-HSD2 can also inhibit 11β-HSD1 actvity (13) and compromise endothelial barrier by interacting with tight junction proteins (14). Therefore we have investigated the underlying mechanism in *Apoe*$^{-/-}$*Hsd11b2*$^{-/-}$ double-knockout (E/b2) mice, lacking both apolipoprotein E and 11β-HSD2.

Materials and Methods

Generation of ApoE/Hsd11b2 Double-Knockout Animals

All animal studies were conducted in accordance with the National Institutes of Health guidelines for the Care and Use of Laboratory Animals under the auspices of the Animals (Scientific Procedures) Act UK 1986 following prior approval by the local ethical committee. The previously targeted Hsd11b2 allele (9) was transferred to C57BL/6J by 9 generations of consecutive backcrosses. Two C57Bl/6J females homozygous for deletion of the Hsd11b2 allele were crossed with an Apoe-knockout (*Apoe*$^{-/-}$) male on the C57Bl/6J background (Charles River, France) derived from the original knockout line (15). Double heterozygous male offspring (Apoe$^{+/-}$/Hsd11b2$^{+/-}$) were backcrossed to *Apoe*$^{-/-}$ females; progeny were subsequently inter-crossed to produce double homozygous knockout animals (*Apoe*$^{-/-}$/Hsd11b2$^{-/-}$). The colony was maintained by crossing homozygous *Apoe*$^{-/-}$/Hsd11b2$^{-/-}$ knockout males (E/b2) to *Apoe*$^{-/-}$/Hsd11b2$^{+/-}$ females; double knockout E/b2 progeny were selected for experimental protocols. Genotyping was performed by PCR using genomic DNA extracted from ear clips. *Apoe* primers were located outside the neo cassette inserted into exons 3 and 4 (ApoEex3f: AAC TTA CTC TAC ACA GGA TGC C; *Apoe* ex4r: CGT CAT AGT GTC CTC CAT CAG TGC). These primers amplify both the wild type allele (584 bp) and the knockout allele (1500 bp). PCR conditions were: denaturation at 94°C for 5 min, then 3 min of elongation at 72°C, followed by 32 cycles of 94°C for 30 s, 58°C for 1 min, and 72°C for 2 min. The Hsd11b2 allele (981bp) was amplified with primers 11b2_679f: AGG CTG ATG ATA GAT TCA CGA GAC and 11b2_1660r: CGA

Europe PMC Funders Author Manuscripts

Europe PMC Funders Author Manuscripts

ATG TGT CCA TAA GCA GTG. The knockout allele was amplified using the genomic primer 11b2_679f (above) and primer Neof1441: GCG AAT GGG CTG ACC GCT TCC TCG, complementary to the Neo gene sequence in the targeting cassette inserted in the reverse orientation.

Animal Treatments

Male *Apoe*$^{-/-}$ and E/b2 mice were maintained on normal chow diet with water ad libitum and a 12h:12h light:dark cycle. Systolic blood pressure was measured in conscious, restrained mice by non-invasive tail cuff plethysmography (16). This procedure was repeated on a weekly basis during the first month followed by monthly measurements until termination. Representative *Apoe*$^{-/-}$ and E/b2 mice were killed by asphyxiation with CO_2 at age 3 and 6 months for assessment of atherosclerotic lesion formation. To evaluate the effects of drugs, 2 month-old male E/b2 and *Apoe*$^{-/-}$ mice were randomized to receive normal chow diet containing the MR antagonist eplerenone (200 mg/kg/day), the epithelial sodium channel blocker amiloride (1 mg/kg/day; n=9) that acts downstream of renal MR to lower blood pressure (17), or vehicle for 3 months.

Tissue Preparation for Assessment of Atherosclerosis

Following euthanasia the vasculature was perfusion-fixed in situ with 10% neutral buffered paraformaldehyde via the left ventricle. Arteries removed included the aorta and the following major branches: brachiocephalic (inominate) artery and its branches, the right subclavian and right common carotid arteries, the left common carotid and left subclavian arteries, and the major branches of the abdominal aorta including the celiac, superior mesenteric arteries and the renal arteries.

Semi-Quantitative Gross Assessment of Atherosclerosis in the Arterial Tree

Adventitia were dissected from fixed arteries under a dissecting microscope. Atherosclerotic lesions were visualized through the translucent arterial wall as yellowish-white opaque deposits. A semi-quantitative scoring system was applied for atherosclerotic deposits at the following sites: (i) lesser curvature of the aortic arch; (ii) origins of principal branches of thoracic aorta (brachiocephalic, left common carotid and left subclavian arteries); (iii) origin of right and distal right and left common carotid arteries; (iv) distal right and left subclavian arteries; and (v) principal branches of abdominal aorta (celiac, superior mesenteric and renal arteries). Scoring was based on the following criteria: 0 = absent; 1= trace; 2 = mild; 3= moderate; and 4 = severe.

Arterial trees from all mice of both genotypes were coded and read blind by two independent observers. For each site the arterial tree with the most severe deposit was assigned a score of 4. The remaining coded arterial trees were then assigned a score based on that sample.

Quantification of Atherosclerotic Lesion Size

The brachiocephalic artery was dissected out to provide a Y-shaped piece of vessel containing the origins of the subclavian and carotid arteries; this was embedded in paraffin. Serial sections (3 μm) were taken from the proximal 60 μm of the brachiocephalic artery once the leaflets of the aortic arch were no longer visible. Sections were stained with US Trichrome; plaque sizes were quantified by light microscopy (Zeiss Axioscop, 10x magnification) with computerized planimetry (MCID Basic 7.0 image analysis software; Imaging Research Inc, Brock University, St Catherines, Ontario, Canada). The area inside the internal elastic lamina was subtracted from the area inside the external elastic lamina to

Europe PMC Funders Author Manuscripts

Europe PMC Funders Author Manuscripts

provide a measure of media area. Subclavian arteries from randomly-selected mice in the drug study were also paraffin embedded and sectioned as above for morphometric studies.

Immunohistochemistry

Plaque collagen content was assessed by Picrosirius red staining and extracellular lipid content by quantification of the holes left behind during histological processing of UST stained sections (18). Plaque macrophage and smooth muscle cell content was assessed using Mac-2 (VH BIO, Gateshead, UK) and smooth muscle α-actin (Sigma, Poole, UK) antibodies, respectively. Vascular cell adhesion molecule (VCAM-1) (Cambridge Biosciences, Cambridge, UK) antibody was used to investigate adhesion molecule expression. Staining was imaged using a light microscope (Zeiss Axioskop) coupled to a Photometrics CoolSnap camera (Tucson, U.S.A.). Photoshop CS3 Extended software was used to quantify staining and data are expressed as stained areas relative to total plaque size (percentage). A semi-quantitative scoring method (carried out blind to genotype) was employed to assess VCAM-1 expression where an arbitrary score of 0-4 was given to each section based on the % of the circumference of the specific endothelial staining.

Cell Culture

Mouse aortic endothelial cells (MAEC cell line) (19) were maintained in Endothelial Basal Medium 2 (EBM-2) (Lonza, Slough, UK) supplemented with 10% FCS and Pen/Strep. Cells were treated overnight in serum-free medium with one of the following; 10ng/ml TNF-α (Santa Cruz Biotechnology, Santa Cruz, California, USA), 1nM aldosterone in the presence/absence of 1μM spironolactone, 1nM corticosterone in the presence/absence of 1μM glycyrrhetinic acid and 1μM spironalactone (all from Sigma, Poole, UK). VCAM-1 expression was quantified by counting the number of positively stained cells per field (at x40 magnification) in four separate fields for each treatment.

Plasma lipid and Lipoprotein Analysis

Terminal blood samples were taken for lipid analysis from the left ventricle of vehicle- and drug-treated E/b2 and *Apoe*$^{-/-}$ mice. Total plasma cholesterol was measured by a colorimetric reaction using the Cholesterol/Cholesteryl Ester Quantification kit (Merck)

Statistical Analyses

Data was analysed by the GraphPad Prism analysis package. (San Diego, CA). Data are expressed as means ± SEM. For analysis of unpaired data sets, Student's unpaired *t*-test was used for comparison of 2 groups and one-way ANOVA with Tukey's *post hoc* test was used for more than 2 groups. Repeated measures ANOVA was used for comparison of matched data sets. Two-way ANOVA followed by Bonferroni post hoc tests was used for analysing the effects of drug treatments between groups. Scored data were analysed by a non-parametric Kruskal-Wallis one-way ANOVA followed by Dunn's *post hoc* test. A value of $P<0.05$ was considered to be statistically significant.

Results

Double-knockout Apoe$^{-/-}$Hsd11b2$^{-/-}$ (E/b2) mice show accelerated atherosclerosis

E/b2 mice were born in the expected Mendelian numbers to *Apoe*$^{-/-}$*HSD11b2*$^{+/-}$ females mated with E/b2 males and showed no difference in weight gain to *Apoe*$^{-/-}$ *HSD11b2*$^{+/-}$ littermates or age-matched *Apoe*$^{-/-}$ mice.

At 3 months of age, *Apoe*$^{-/-}$ mice raised on a standard chow diet displayed few, if any, signs of atherosclerosis in the brachiocephalic artery (Figure 1a). In contrast, by 3 months of

Europe PMC Funders Author Manuscripts

Europe PMC Funders Author Manuscripts

age on the same diet, E/b2 mice lacking both 11β-HSD2 and apolipoprotein E, displayed atheroma (lipid core and proliferating smooth muscle cells) with occasional thin fibrous caps, affecting the aortic arch and its major branches, including the brachiocephalic trunk (Figure 1a), a site particularly susceptible to plaque development in these animals when fed an atherogenic 'western' diet (20). At 3 months some severe lesions were already present in E/b2 mice, with extended necrotic areas, cholesterol clefts, neointimal expansion, and elastic lamina remodeling.

By 6 months of age, E/b2 mice displayed complex severe atherosclerotic lesions with multiple fibrous caps (Figure 1b). Importantly, these included buried caps, which have been suggested as being indicative of earlier plaque instability (21) (Figure 1b, Table 1). However, in 6 month-old *Apoe*$^{-/-}$ mice raised on the same chow diet, atherosclerosis remained sporadic (only one of the 6 animals in this group had a notable plaque; example shown in Figure 1b) in the brachiocephalic artery (Figure 1b). This remarkable increase in atherosclerosis with 11β-HSD2-deficiency was despite similar plasma cholesterol levels between E/b2 (306±54 mg/dl) and *Apoe*$^{-/-}$ (288±46 mg/dl) mice.

Quantitative analysis of the areas inside the external elastic lamina (EEL), lesion areas, and lumen areas of the brachiocephalic artery revealed significantly larger atherosclerotic lesions in E/b2 mice at 3 and 6 months of age compared to age-matched *Apoe*$^{-/-}$ mice, as well as a significant reduction of lumen size relative to the size of the vessel (Figure 1c and Table 1). There was also a significant reduction of lumen size relative to the size of the vessel, although the absolute lumen size was maintained (vessel diameter was also increased) (Figure 1 and Table 1), suggestive of expansive remodeling in E/b2 mice.

Plaque composition is altered in E/b2 mice

Immunohistochemical staining revealed that atherosclerotic plaques in brachiocephalic arteries of 6 month-old E/b2 mice contained dense accumulations of macrophages and foam cells (Figure 2a), most notably at the 'shoulder' of lesions and near buried fibrous caps. Macrophage infiltration (Figure 2b), and lipid content of plaques (Figure 2c) were both significantly greater in E/b2 than in *Apoe*$^{-/-}$ mice. Furthermore, plaques in 3 month-old Eb/2 mice contained significantly more macrophages (Figure 2b) and lipid (Figure 2c) than those in plaque size-matched *Apoe*$^{-/-}$ counterparts (examples of rare plaques from 6 month-old *Apoe*$^{-/-}$ mice selected to show composition). Smooth muscle cell (SMC) content of plaques, assessed by α-smooth muscle actin (SMA) immunoreactivity, did not differ between E/b2 and *Apoe*$^{-/-}$ mice (Figure 2d). Picrosirius red staining of collagen was significantly lower in plaques from 3 and 6 month-old E/b2 mice compared to plaques from 6 months old *Apoe*$^{-/-}$ mice (Figure 2e). Thus, 11β-HSD2-deficiency promotes the formation of collagen-poor, lipid- and macrophage-rich plaques, suggestive of a "vulnerable" plaque phenotype.

Accelerated atherosclerosis in E/b2 mice is associated with increased expression of VCAM-1

VCAM-1 immunoreactivity was significantly higher in unaffected areas of brachiocephalic artery endothelium in both 3 months-old and 6 months-old E/b2 mice compared to age matched *Apoe*$^{-/-}$ controls (Figure 3) both in the endothelium covering the plaque and in plaque-free regions of the vessel wall. Importantly, comparison of similar-sized vessels from 3 month-old E/b2 mice and 6 month-old *Apoe*$^{-/-}$ mice showed significantly higher VCAM-1 expression in E/b2 mice, despite their younger age (Figure 3a,b).

Europe PMC Funders Author Manuscripts

Europe PMC Funders Author Manuscripts

Atheroprotective effects of eplerenone and amiloride do not correlate with their ability to lower blood pressure

As anticipated from the previously reported phenotype of *Hsd11b2*$^{-/-}$ mice, (9) E/b2 animals were moderately hypertensive compared with *Apoe*$^{-/-}$ mice, most likely due to over-activation of MR in the kidney (systolic blood pressure 141.8±2.5 mmHg in E/b2 mice versus 112.6±1.7 mmHg in *Apoe*$^{-/-}$ mice; $P<0.001$). Thus, the exacerbated atherosclerosis in E/b2 mice could be attributable to hypertension as a result of renal MR activation by glucocorticoids, or to a direct effect of 11β-HSD2-deficiency within the vascular wall or a combination of these factors. To address MR involvement and to determine the dependency of the phenotype on hypertension, 2-month old mice were fed chow diet containing vehicle or one of two pharmacologic inhibitors for 3 months; amiloride, an epithelial sodium channel blocker that acts downstream of renal MR to lower blood pressure, and eplerenone, a highly-selective MR antagonist. The dose chosen for the latter (200 mg/kg/day in chow) was previously shown to reduce atheroma formation in *Apoe*$^{-/-}$ mice administered aldosterone (22). We found no effect of any drug treatment on blood pressure of *Apoe*$^{-/-}$ mice (not shown). Eplerenone had no significant effect on systolic blood pressure in E/b2 mice while amiloride reduced it by ~11 mmHg, almost halving the blood pressure difference between E/b2 and *Apoe*$^{-/-}$ mice (Figure 4a). However, being less effective as a hypotensive drug, eplerenone was more effective than amiloride in reducing overall plaque score as estimated by blinded, semi-quantitative scoring assessed across 5 sites (Figure 4b,c). Quantitative histological analysis showed that eplerenone also dramatically reduced plaque size and the expansive remodeling in subclavian arteries which are particularly prone to large occlusive plaques in E/b2 mice (Figure 4d,e). Both eplerenone and amiloride reduced lesion size in brachiocephalic arteries (Figure 4f,g and Table 2). The pattern of expansive remodeling evident in untreated E/b2 mice was also reduced following treatment with both eplerenone and amiloride (Table 2). Thus, the stronger atheroprotective effect of eplerenone in comparison with amiloride, with the latter producing a larger reduction in blood pressure, indicates that the predominant mechanism leading to accelerated atherosclerosis in E/b2 mice is unlikely to be attributable simply to hypertension following renal MR activation.

MR activation contributes to the altered plaque composition in E/b2 mice

To investigate whether MR antagonism altered plaque composition in addition to reducing lesion size in E/b2 mice, macrophage infiltration, α-SMA, collagen and lipid content were measured in brachiocephalic plaques of E/b2 mice following 3 months of treatment with eplerenone or vehicle. Macrophage content was significantly reduced by eplerenone treatment (Figure 5a,b). Despite the increase in lipid content of plaques in E/b2 mice compared to *Apoe*$^{-/-}$ mice, MR blockade with eplerenone had no effect on plaque lipid content in E/b2 mice (Figure 5a,c). Surprisingly, whilst there was no difference in plaque α-SMA content between E/b2 and *Apoe*$^{-/-}$ mice, smooth muscle cell content was significantly increased by MR blockade in E/b2 mice (Figure 5a,d). Eplerenone treatment also significantly increased plaque collagen content compared to vehicle-treated E/2b mice (Figure 5a,e). There was a trend towards a reduction in the incidence of buried fibrous caps in the brachiocephalic artery of eplerenone-treated E/b2 mice (1.10±0.31 buried caps for vehicle-treated *vs* 0.56±0.18 for eplerenone-treated E/b2 mice.

Glucocorticoids in the presence of 11β-HSD2 inhibitor cause MR mediated up regulation of VCAM-1 expression in vitro

Mouse aortic endothelial cells (MAEC) were used to test whether mineralocorticoids or glucocorticoids acting through MR can affect VCAM-1 expression and whether 11β-HSD2 inhibition may be important in regulation of MR specificity. Similar to TNF-α which potently increases VCAM-1 expression in endothelial cells (23), aldosterone markedly

Europe PMC Funders Author Manuscripts

Europe PMC Funders Author Manuscripts

increased the number of MAEC expressing VCAM-1 (>7-fold; Figure 6), an effect blocked by pre-treatment with the MR antagonist, spironolactone, suggesting an MR-mediated mechanism. Corticosterone alone had no effect on VCAM-1 expression. However, inhibition of 11β-HSD2 by pre-treatment with glycyrrhetinic acid (a widely used 11β-HSD inhibitor (24), which had no effect on VCAM-1 expression on its own, allowed corticosterone to induce a >9-fold increase in the number of VCAM-1-stained cells (Figure 6). Using RT PCR we have confirmed that 11β-HSD1 is not expressed in MAEC (data not shown). Thus, in this cell line, as in kidney, 11β-HSD2 protects MR from activation by glucocorticoids. Consistent with MR involvement, VCAM-1 up-regulation by corticosterone in the presence of glycyrrhetinic acid was reversed by blockade of MR with spironolactone (Figure 6b).

Discussion

Early development of severe occlusive atheromatous plaques in E/b2 mice provides a new experimental model of atherosclerosis, mechanistically under-pinned by glucocorticoid-mediated activation of MR. In contrast to most existing models, high fat/western diet is not required for the development of atherosclerosis in Eb/2 mice. Indeed, when fed a chow diet, *Apoe*$^{-/-}$ mice exhibit moderate hyperlipidaemia and only develop mature atheromatous plaques at 8–10 months of age (25). Feeding *Apoe*$^{-/-}$ mice a “western diet” (containing cholesterol) increases plasma cholesterol, induces systemic inflammation and accelerates atherogenesis so that lesions appear within 5 weeks (20). It therefore appears that progressive atherosclerosis in *Apoe*$^{-/-}$ mice is strictly dependent on systemic inflammation and elevated plasma cholesterol associated with the western diet.

Atherogenesis in E/b2 mice was associated with early and increased macrophage infiltration of brachiocephalic lesions, even when matched with similar-sized lesions in older *Apoe*$^{-/-}$ mice. An increase in the number of buried caps in plaques of older E/b2 animals could reflect multiple events of plaque rupture and repair in E/b2 mice, typical of vulnerable plaques. Thus, for investigation of the processes leading to a vulnerable plaque phenotype, E/b2 mice may be a better experimental platform than *Apoe*$^{-/-}$ mice.

The ability of eplerenone administration to reduce plaque size and alter plaque composition implicates MR activation as mechanistically important in accelerating atherosclerosis in E/b2 mice. This is consistent with previous data showing that aldosterone is pro-atherogenic in animal models (23,28) although this has not been replicated in all studies (26). Moreover, eplerenone has beneficial effects on experimental atherosclerosis in non-human primates (27), again implicating MR activation in pathogenesis of atherosclerosis. This raises the possibility that the pro-atherogenic effects of MR activation are through cortisol (a glucocorticoid) rather than the mineralocorticoid, aldosterone.

Crucially, the effect of eplerenone on atherosclerosis in E/b2 mice was independent of MR effects on blood pressure (which was unaltered in E/b2 mice by this modest dose of eplerenone). In the absence of 11β-HSD2, MR are not protected from activation by glucocorticoids and their activation in the distal nephron increases activity of epithelial sodium channels and Na/K ATPase, leading to hypertension (17). The extent of hypertension in E/b2 mice was comparable to that previously reported in single-knockout *Hsd11b2*$^{-/-}$ mice (9). Bypassing MR activation with the epithelial sodium channel blocker amiloride reduced blood pressure in E/b2 mice but was less effective in diminishing atherosclerosis than eplerenone. Hypertension in 11β-HSD2 KO mice is initiated by MR activation and volume expansion, but already after 2.5 months of age activity of eNaC was returned to the basal level and high blood pressure was maintained by activation of alpha 1-adrenergic receptors (28). Hence eplerenone can not effectively normalize blood pressure at

Europe PMC Funders Author Manuscripts

Europe PMC Funders Author Manuscripts

these later stages, while amiloride still can. Another possible contributor to hypertension in HSD11b2 deficiency is the vasoconstrictive effect mediated by glucocorticoid receptors (29,30) which will not be affected by MR inhibitor eplerenone.

Thus, although hypertension may play a part in the accelerated atherogenesis in E/b2 mice there is clearly a component of atherogenesis that is not merely due to the hypertension of 'apparent mineralocorticoid excess' produced by MR over-activation in the distal nephron. This concurs with two previous studies in which blood pressure played little or no role in atherogenesis - in mice deficient for both Apolipoprotein E and eNOS(31) and *Apoe*$^{-/-}$ mice with renovascular hypertension (one kidney one clip and two kidneys/two clips models) (32). In contrast, blood pressure *per se* played only a minor role in atheroma progression in *Apoe*$^{-/-}$ mice with renovascular hypertension as compared to the large effect of angiotensin II (33). Our data implicate activation of non-renal MR in the pathogenesis of accelerated atherogenesis in E/b2 mice with the vascular wall being the most likely candidate site. In humans, 11β-HSD2 immunoreactivity has been reported in arterioles and veins (34) with immunoreactivity and enzyme activity concentrated in endothelial cells (35). Both 11β-HSD2 mRNA and enzyme activity are found in rodent vessels, most likely including the endothelium (36). Consistent with co-localisation of MR and 11β-HSD2 in endothelial cells, MAEC *in vitro* also have functional MR and 11β-HSD2. *In vitro,* activation of MR by aldosterone increases leukocyte adhesion molecules in primary human endothelial cells from umbilical cord (37). It was shown recently that aldosterone stimulates transcription of the proatherogenic leukocyte-endothelial cell adhesion proteins in human coronary artery and aortic ECs. In the same study, inhibition of 11β-HSD2 enhanced cortisol-induced transcription of a reporter transgene mediated by MR in aortic endothelial cells (38). We show that VCAM-1 expression was increased *in vivo* in E/b2 mice in affected and unaffected regions of the brachiocephalic artery. A direct effect of MR in this increase (rather than an effect of shear stress) is supported by the MR-dependent potent increase in VCAM-1 expression in MAECs treated with aldosterone or with corticosterone in the presence of an 11β-HSD2 inhibitor. VCAM-1 increases monocyte/macrophage adhesion to endothelial cells (39) and is mechanistically linked to inflammatory processes (40) and atheroma development in *Apoe*$^{-/-}$ (41) and LDL$^{-/-}$ mice (42). Increased expression of VCAM-1 in E/b2 mice may be responsible for the increased macrophage infiltration leading to accelerated atherogenesis and may also stimulate expansive vessel remodeling (43).

Overall, these findings indicate that loss of function of 11β-HSD2 leads to striking atherogenesis in E/b2 mice mediated by activation of non-renal MR. Endothelial expression of VCAM-1 and massive infiltration of the atherosclerotic plaques by macrophages at moderately elevated levels of plasma cholesterol are the characteristic features of this new mouse model of atherosclerosis.

We have shown for the first time that 11β-HSD2 is atheroprotective. In its absence activation of MR mainly by glucocorticoids enhances inflammatory processes in the atherosclerotic plaque. This effect of MR is not solely attributable to changes in blood pressure. Whether it is associated with the altered activation mechanisms of MR in the endothelium remains to be investigated in the future experiments with tissue specific knockout of MR.

Acknowledgments

This work was supported by a project grant from the British Heart Foundation. Ms. Lorna Whiteside contributed to pilot work. We are grateful to Dr.G.A.Gray for discussions and useful suggestions. Asim Azfer confirmed absence of 11β-HSD1 mRNA in the MAEC cell line.

Grant Support: YK(PI), GD, PWH, JRS, DB and DJW were recipients of the British Heart Foundation Project Grant PG/05/007/18240. DM was the recipient of a Wellcome Trust PhD fellowship 078823/Z/05/Z. JJM was the recipient of a Wellcome Trust Principal Research Fellowship. LW was the recipient of a Wellcome Trust vacation scholarship.

References

1. Pitt B, Zannad F, Remme WJ, Cody R, Castaigne A, Perez A, Palensky J, Wittes J. The effect of spironolactone on morbidity and mortality in patients with severe heart failure. Randomized Aldactone Evaluation Study Investigators. N Engl J Med. 1999; 341:709–717. [PubMed: 10471456]
2. Pitt B, Williams G, Remme W, Martinez F, Lopez-Sendon J, Zannad F, Neaton J, Roniker B, Hurley S, Burns D, Bittman R, Kleiman J. The EPHESUS trial: eplerenone in patients with heart failure due to systolic dysfunction complicating acute myocardial infarction. Eplerenone Post-AMI Heart Failure Efficacy and Survival Study. Cardiovasc Drugs Ther. 2001; 15:79–87. [PubMed: 11504167]
3. Connell JM, Davies E. The new biology of aldosterone. J Endocrinol. 2005; 186:1–20. [PubMed: 16002531]
4. Arriza JL, Weinberger C, Cerelli G, Glaser TM, Handelin BL, Housman DE, Evans RM. Cloning of human mineralocorticoid receptor complementary DNA: structural and functional kinship with the glucocorticoid receptor. Science. 1987; 237:268–275. [PubMed: 3037703]
5. Walker BR. Glucocorticoids and cardiovascular disease. European journal of endocrinology / European Federation of Endocrine Societies. 2007; 157:545–559. [PubMed: 17984234]
6. Stewart PM, Corrie JE, Shackleton CH, Edwards CR. Syndrome of apparent mineralocorticoid excess. A defect in the cortisol-cortisone shuttle. J Clin Invest. 1988; 82:340–349. [PubMed: 3164727]
7. Wilson RC, Krozowski ZS, Li K, Obeyesekere VR, Razzaghy-Azar M, Harbison MD, Wei JQ, Shackleton CH, Funder JW, New MI. A mutation in the HSD11B2 gene in a family with apparent mineralocorticoid excess. J Clin Endocrinol Metab. 1995; 80:2263–2266. [PubMed: 7608290]
8. Edwards CR, Stewart PM, Burt D, Brett L, McIntyre MA, Sutanto WS, de Kloet ER, Monder C. Localisation of 11 beta-hydroxysteroid dehydrogenase--tissue specific protector of the mineralocorticoid receptor. Lancet. 1988; 2:986–989. [PubMed: 2902493]
9. Kotelevtsev Y, Brown RW, Fleming S, Kenyon C, Edwards CR, Seckl JR, Mullins JJ. Hypertension in mice lacking 11beta-hydroxysteroid dehydrogenase type 2. J Clin Invest. 1999; 103:683–689. [PubMed: 10074485]
10. Fantidis P. The role of the stress-related anti-inflammatory hormones ACTH and cortisol in atherosclerosis. Current vascular pharmacology. 2010; 8:517–525. [PubMed: 19485904]
11. Walker BR. Cortisol--cause and cure for metabolic syndrome? Diabet Med. 2006; 23:1281–1288. [PubMed: 17116176]
12. Takeda Y, Miyamori I, Yoneda T, Iki K, Hatakeyama H, Blair IA, Hsieh FY, Takeda R. Production of aldosterone in isolated rat blood vessels. Hypertension. 1995; 25:170–173. [PubMed: 7843766]
13. Vicker N, Su X, Lawrence H, Cruttenden A, Purohit A, Reed MJ, Potter BV. A novel 18 beta-glycyrrhetinic acid analogue as a potent and selective inhibitor of 11 beta-hydroxysteroid dehydrogenase 2. Bioorganic & medicinal chemistry letters. 2004; 14:3263–3267. [PubMed: 15149687]
14. Nagasawa K, Chiba H, Fujita H, Kojima T, Saito T, Endo T, Sawada N. Possible involvement of gap junctions in the barrier function of tight junctions of brain and lung endothelial cells. Journal of cellular physiology. 2006; 208:123–132. [PubMed: 16547974]
15. Zhang SH, Reddick RL, Piedrahita JA, Maeda N. Spontaneous hypercholesterolemia and arterial lesions in mice lacking apolipoprotein E. Science. 1992; 258:468–471. [PubMed: 1411543]
16. Krege JH, Hodgin JB, Hagaman JR, Smithies O. A noninvasive computerized tail-cuff system for measuring blood pressure in mice. Hypertension. 1995; 25:1111–1115. [PubMed: 7737724]
17. Rossier BC, Pradervand S, Schild L, Hummler E. Epithelial sodium channel and the control of sodium balance: interaction between genetic and environmental factors. Annual review of physiology. 2002; 64:877–897.

Europe PMC Funders Author Manuscripts
Europe PMC Funders Author Manuscripts

Europe PMC Funders Author Manuscripts

18. Johnson J, Carson K, Williams H, Karanam S, Newby A, Angelini G, George S, Jackson C. Plaque rupture after short periods of fat feeding in the apolipoprotein E-knockout mouse: model characterization and effects of pravastatin treatment. Circulation. 2005; 111:1422–1430. [PubMed: 15781753]
19. Nishiyama T, Mishima K, Ide F, Yamada K, Obara K, Sato A, Hitosugi N, Inoue H, Tsubota K, Saito I. Functional analysis of an established mouse vascular endothelial cell line. J Vasc Res. 2007; 44:138–148. [PubMed: 17215585]
20. Nakashima Y, Plump AS, Raines EW, Breslow JL, Ross R. ApoE-deficient mice develop lesions of all phases of atherosclerosis throughout the arterial tree. Arterioscler Thromb. 1994; 14:133–140. [PubMed: 8274468]
21. Williams H, Johnson JL, Carson KG, Jackson CL. Characteristics of intact and ruptured atherosclerotic plaques in brachiocephalic arteries of apolipoprotein E knockout mice. Arterioscler Thromb Vasc Biol. 2002; 22:788–792. [PubMed: 12006391]
22. Keidar S, Kaplan M, Pavlotzky E, Coleman R, Hayek T, Hamoud S, Aviram M. Aldosterone administration to mice stimulates macrophage NADPH oxidase and increases atherosclerosis development: a possible role for angiotensin-converting enzyme and the receptors for angiotensin II and aldosterone. Circulation. 2004; 109:2213–2220. [PubMed: 15123520]
23. Osborn L, Hession C, Tizard R, Vassallo C, Luhowskyj S, Chi-Rosso G, Lobb R. Direct expression cloning of vascular cell adhesion molecule 1, a cytokine-induced endothelial protein that binds to lymphocytes. Cell. 1989; 59:1203–1211. [PubMed: 2688898]
24. Stewart PM, Krozowski ZS. 11 beta-Hydroxysteroid dehydrogenase. Vitamins and hormones. 1999; 57:249–324. [PubMed: 10232052]
25. Reddick RL, Zhang SH, Maeda N. Atherosclerosis in mice lacking apo E. Evaluation of lesional development and progression. Arterioscler Thromb. 1994; 14:141–147. [PubMed: 8274470]
26. Cassis LA, Helton MJ, Howatt DA, King VL, Daugherty A. Aldosterone does not mediate angiotensin II-induced atherosclerosis and abdominal aortic aneurysms. Br J Pharmacol. 2005; 144:443–448. [PubMed: 15655500]
27. Takai S, Jin D, Muramatsu M, Kirimura K, Sakonjo H, Miyazaki M. Eplerenone inhibits atherosclerosis in nonhuman primates. Hypertension. 2005; 46:1135–1139. [PubMed: 16203870]
28. Bailey MA, Paterson JM, Hadoke PW, Wrobel N, Bellamy CO, Brownstein DG, Seckl JR, Mullins JJ. A switch in the mechanism of hypertension in the syndrome of apparent mineralocorticoid excess. J Am Soc Nephrol. 2008; 19:47–58. [PubMed: 18032795]
29. Goodwin JE, Zhang J, Geller DS. A critical role for vascular smooth muscle in acute glucocorticoid-induced hypertension. J Am Soc Nephrol. 2008; 19:1291–1299. [PubMed: 18434569]
30. Goodwin JE, Zhang J, Velazquez H, Geller DS. The glucocorticoid receptor in the distal nephron is not necessary for the development or maintenance of dexamethasone-induced hypertension. Biochem Biophys Res Commun. 2010; 394:266–271. [PubMed: 20188070]
31. Chen J, Kuhlencordt PJ, Astern J, Gyurko R, Huang PL. Hypertension does not account for the accelerated atherosclerosis and development of aneurysms in male apolipoprotein e/endothelial nitric oxide synthase double knockout mice. Circulation. 2001; 104:2391–2394. [PubMed: 11705813]
32. Mazzolai L, Korber M, Bouzourene K, Aubert JF, Nussberger J, Stamenkovic I, Hayoz D. Severe hyperlipidemia causes impaired renin angiotensin system function in apolipoprotein E deficient mice. Atherosclerosis. 2006; 186:86–91. [PubMed: 16112122]
33. Mazzolai L, Duchosal MA, Korber M, Bouzourene K, Aubert JF, Hao H, Vallet V, Brunner HR, Nussberger J, Gabbiani G, Hayoz D. Endogenous angiotensin II induces atherosclerotic plaque vulnerability and elicits a Th1 response in ApoE−/− mice. Hypertension. 2004; 44:277–282. [PubMed: 15302839]
34. Smith RE, Little PJ, Maguire JA, Stein-Oakley AN, Krozowski ZS. Vascular localization of the 11 beta-hydroxysteroid dehydrogenase type II enzyme. Clin Exp Pharmacol Physiol. 1996; 23:549–551. [PubMed: 8800581]
35. Jang C, Obeyesekere VR, Dilley RJ, Krozowski Z, Inder WJ, Alford FP. Altered activity of 11beta-hydroxysteroid dehydrogenase types 1 and 2 in skeletal muscle confers metabolic

protection in subjects with type 2 diabetes. J Clin Endocrinol Metab. 2007; 92:3314–3320. [PubMed: 17519316]

36. Christy C, Hadoke PW, Paterson JM, Mullins JJ, Seckl JR, Walker BR. 11beta-hydroxysteroid dehydrogenase type 2 in mouse aorta: localization and influence on response to glucocorticoids. Hypertension. 2003; 42:580–587. [PubMed: 12925564]
37. Krug AW, Kopprasch S, Ziegler CG, Dippong S, Catar RA, Bornstein SR, Morawietz H, Gekle M. Aldosterone rapidly induces leukocyte adhesion to endothelial cells: a new link between aldosterone and arteriosclerosis? Hypertension. 2007; 50:e156–157. [PubMed: 17893423]
38. Caprio M, Newfell BG, la Sala A, Baur W, Fabbri A, Rosano G, Mendelsohn ME, Jaffe IZ. Functional mineralocorticoid receptors in human vascular endothelial cells regulate intercellular adhesion molecule-1 expression and promote leukocyte adhesion. Circ Res. 2008; 102:1359–1367. [PubMed: 18467630]
39. Ramos CL, Huo Y, Jung U, Ghosh S, Manka DR, Sarembock IJ, Ley K. Direct demonstration of P-selectin- and VCAM-1-dependent mononuclear cell rolling in early atherosclerotic lesions of apolipoprotein E-deficient mice. Circ Res. 1999; 84:1237–1244. [PubMed: 10364560]
40. Huo Y, Hafezi-Moghadam A, Ley K. Role of vascular cell adhesion molecule-1 and fibronectin connecting segment-1 in monocyte rolling and adhesion on early atherosclerotic lesions. Circ Res. 2000; 87:153–159. [PubMed: 10904000]
41. Dansky HM, Barlow CB, Lominska C, Sikes JL, Kao C, Weinsaft J, Cybulsky MI, Smith JD. Adhesion of monocytes to arterial endothelium and initiation of atherosclerosis are critically dependent on vascular cell adhesion molecule-1 gene dosage. Arterioscler Thromb Vasc Biol. 2001; 21:1662–1667. [PubMed: 11597942]
42. Cybulsky MI, Iiyama K, Li H, Zhu S, Chen M, Iiyama M, Davis V, Gutierrez-Ramos JC, Connelly PW, Milstone DS. A major role for VCAM-1, but not ICAM-1, in early atherosclerosis. J Clin Invest. 2001; 107:1255–1262. [PubMed: 11375415]
43. Brown NJ. Aldosterone and vascular inflammation. Hypertension. 2008; 51:161–167. [PubMed: 18172061]

Europe PMC Funders Author Manuscripts

Europe PMC Funders Author Manuscripts

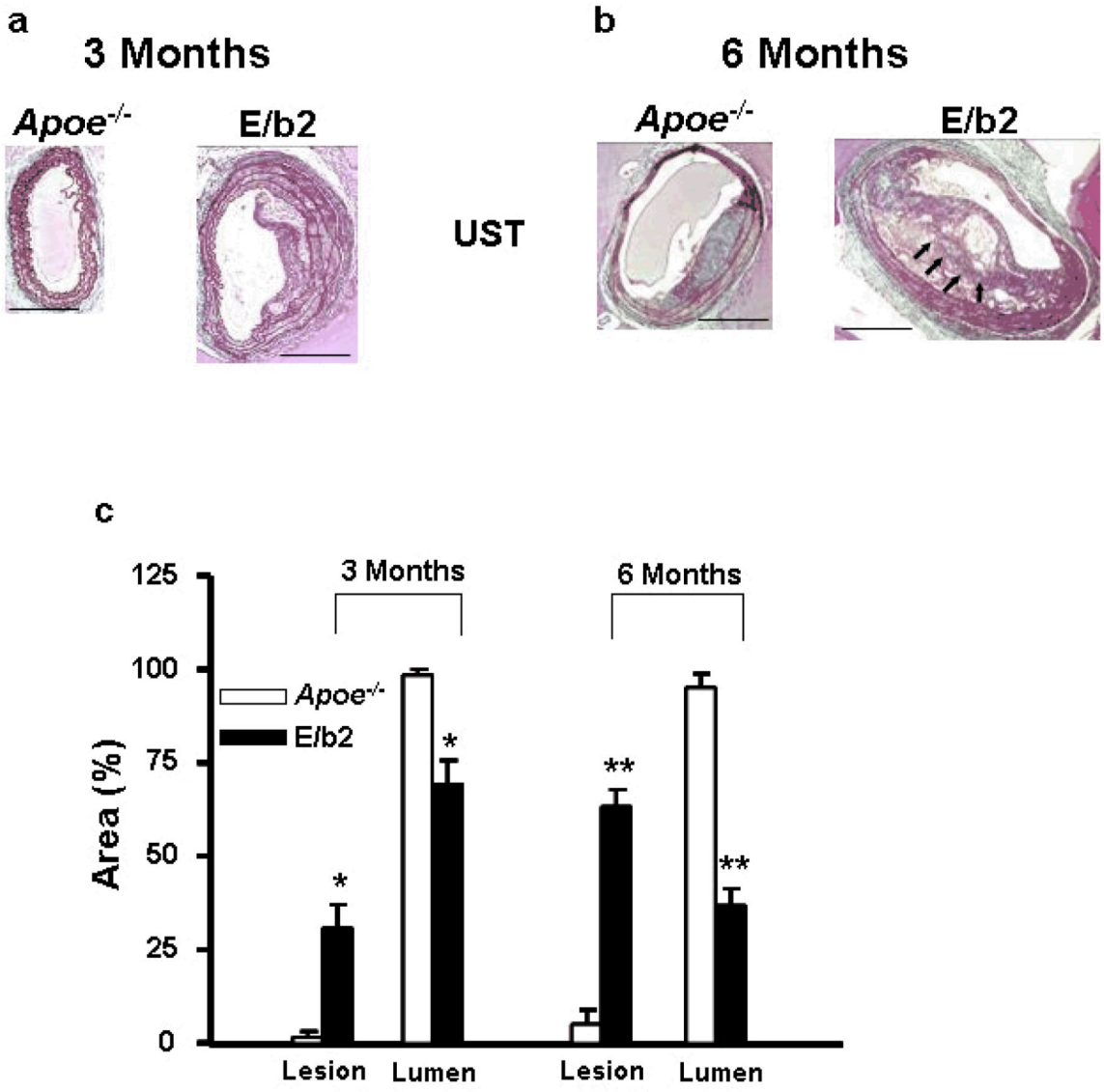

Figure 1. Accelerated atherosclerosis in *Apoe*$^{-/-}$ mice on a standard low-fat diet

(a) Atherosclerotic lesions and outward remodeling were evident in the brachiocephalic arteries of 3 month old E/b2 mice but not in *Apoe*$^{-/-}$ mice (US trichrome stain; Magnification x10). (b) At 6 months of age, lesion development and outward remodeling were significantly greater in E/b2 than in *Apoe*$^{-/-}$ mice. The example used for *Apoe*$^{-/-}$ shows the largest plaque seen at this age (US trichrome stain; Magnification x10). Lesions in E/b2 were more complex with evidence of buried fibrous caps (black arrows). Scale bar = 250 μm

(c) Quantitative analysis confirmed that lesion sizes were increased and lumens were reduced in E/b2 mice compared with *Apoe*$^{-/-}$ mice. Data are means ± SEM. *, $P<0.05$; **, $P<0.01$ compared with *Apoe*$^{-/-}$ using Student's unpaired t-test (n=4–8).

Europe PMC Funders Author Manuscripts
Europe PMC Funders Author Manuscripts

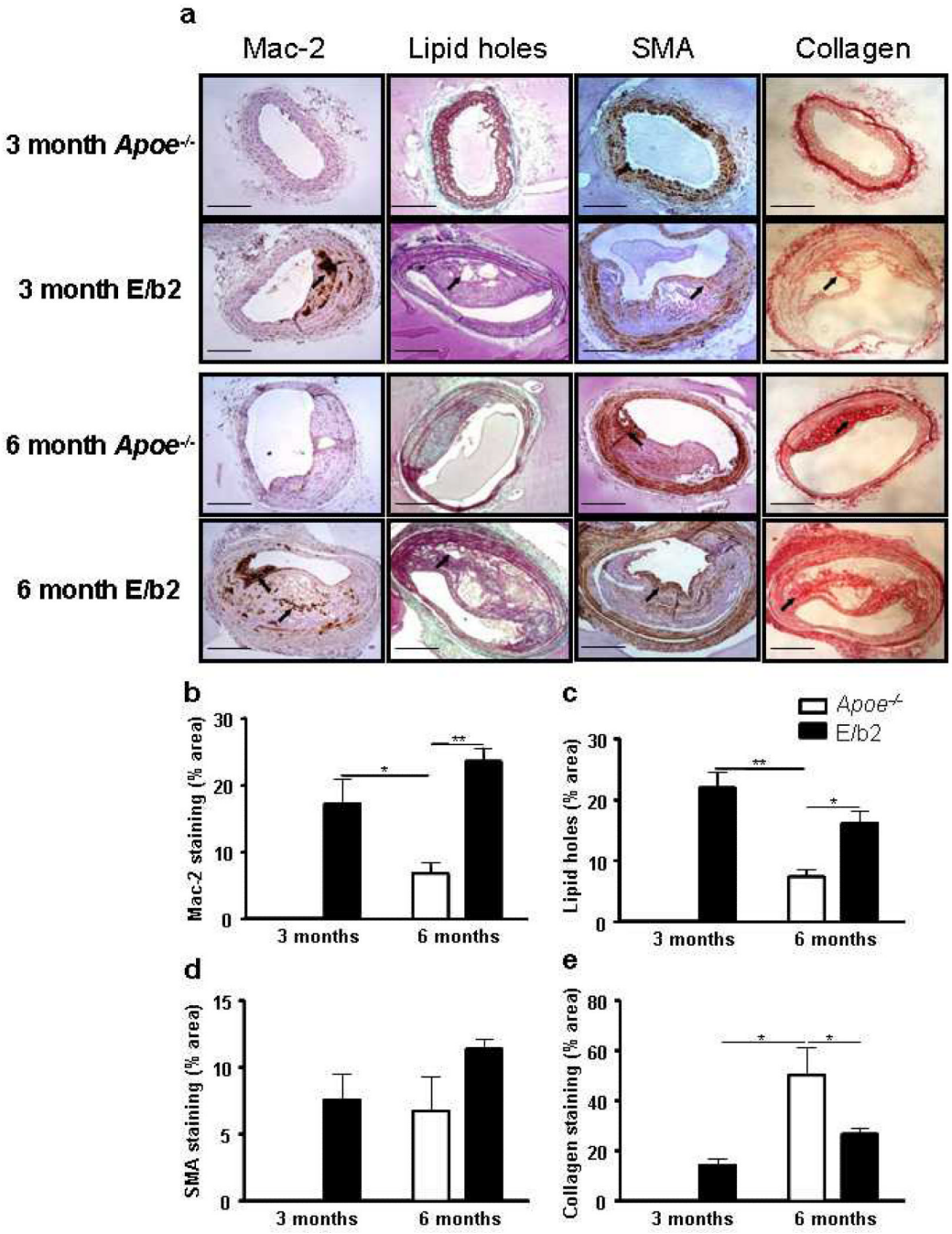

Figure 2. Accelerated atherosclerosis in E/b2 mice is associated with macrophage infiltration and altered plaque composition

(a) At 3 months of age *Apoe*$^{-/-}$ mice are lesion free whilst E/b2 mice show macrophage-infiltrated plaques (staining with anti Mac-2 antibodies) with a high lipid and low collagen content. By 6 months, E/b2 mice have large macrophage-rich plaques with a high density of lipids and sparse collagen staining. In comparison, 6 month-old *Apoe*$^{-/-}$ mice have plaques that are rich in collagen and low in lipid and macrophage content. E/b2 and *Apoe*$^{-/-}$ mice at both ages show similar levels of α-SMA and collagen staining indicative of SMC within their plaques. Representative images (of 6 mice/group, except in case of 6 month *Apoe*$^{-/-}$ where uncommon larger plaques were selected to investigate composition) captured at x10

Europe PMC Funders Author Manuscripts
Europe PMC Funders Author Manuscripts

magnification. Arrows indicate regions of interest corresponding to names of each column. Scale bar = 250 μm.

(b)-(e) The area of staining for each plaque component was quantified using Photoshop CS3 Extended software and expressed as a % of total plaque area. Macrophage (b) and lipid (c) content were both increased in brachiocephalic plaques from 3 and 6 month E/b2 mice compared to those from *Apoe*$^{-/-}$ mice at 6 months of age. There was no difference in the α-SMA (d) content of plaques between *Apoe*$^{-/-}$ and E/b2 mice at either 3 or 6 months of age. Collagen (e) content was reduced in brachiocephalic plaques from 3 and 6 month E/b2 mice compared to those from *Apoe*$^{-/-}$ mice at 6 months of age. Data are mean ± sem, n= 5-7/group. Analysed by two-way ANOVA: * $p<0.05$, ** $p<0.005$.

Europe PMC Funders Author Manuscripts

Europe PMC Funders Author Manuscripts

Europe PMC Funders Author Manuscripts

Europe PMC Funders Author Manuscripts

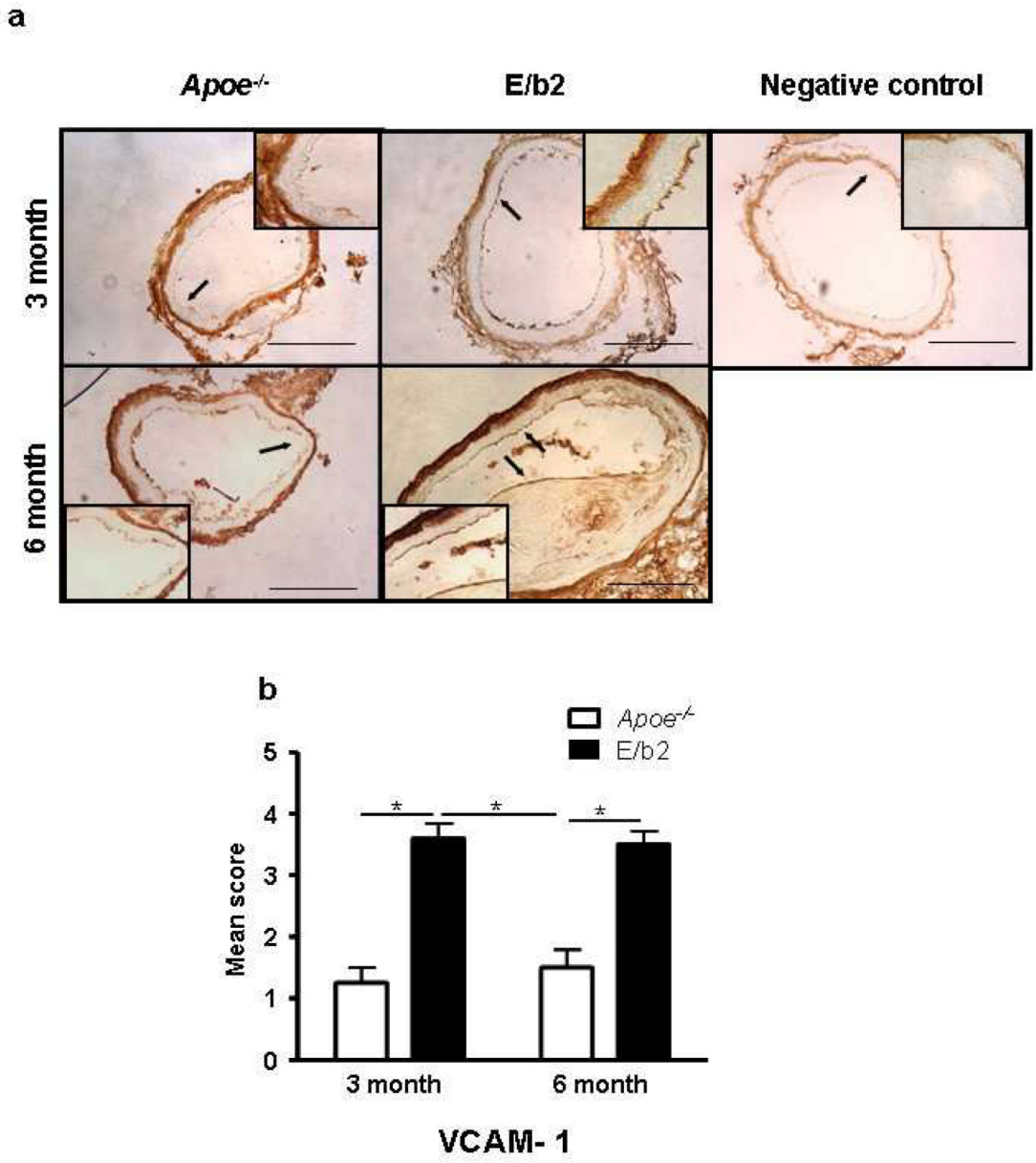

Figure 3. Endothelial cell expression of VCAM-1 is upregulated in E/b2 mice

(a) *Apoe*$^{-/-}$ mice at 3 months show sparse endothelial staining for VCAM-1 (top left panel) while age-matched E/b2 mice have more abundant and intense VCAM-1 immunoreactivity (top middle panel). At 6 months, *Apoe*$^{-/-}$ mice (bottom left panel) show increased VCAM-1 staining compared to 3 month-old *Apoe*$^{-/-}$ mice, but it is still lower than in E/b2 mice (bottom right panel). Arrows indicate specific staining for VCAM-1 in endothelium (highlighted in embedded boxes). Adventitia is stained non-specifically as a result of entrapment of streptavidin-HRP complex (see negative control) Representative images (of 4-6 mice/group) captured at x10 magnification. Scale bar = 250μm.

(b) VCAM-1 staining is significantly greater in endothelium of 3 and 6 month-old E/b2 mice compared to age-matched *Apoe*$^{-/-}$ mice. At 3 months, VCAM-1 expression is higher in E/b2 vessels compared to *Apoe*$^{-/-}$ mice at 6 months with the same size of plaques. Data are means ± sem, n=4-6/group. Analysed by Kruskal-Wallis non-parametric test, *** =

p<0.0001. Scoring: 0=absent; 1= <25% circumference stained; 2= 25-50% circumference stained; 3= 50-75% circumference stained; 4= >75% circumference stained. Scoring: 0=absent; 1= <25% circumference stained; 2= 25-50% circumference stained; 3= 50-75% circumference stained; 4= >75% circumference stained.

Europe PMC Funders Author Manuscripts

Europe PMC Funders Author Manuscripts

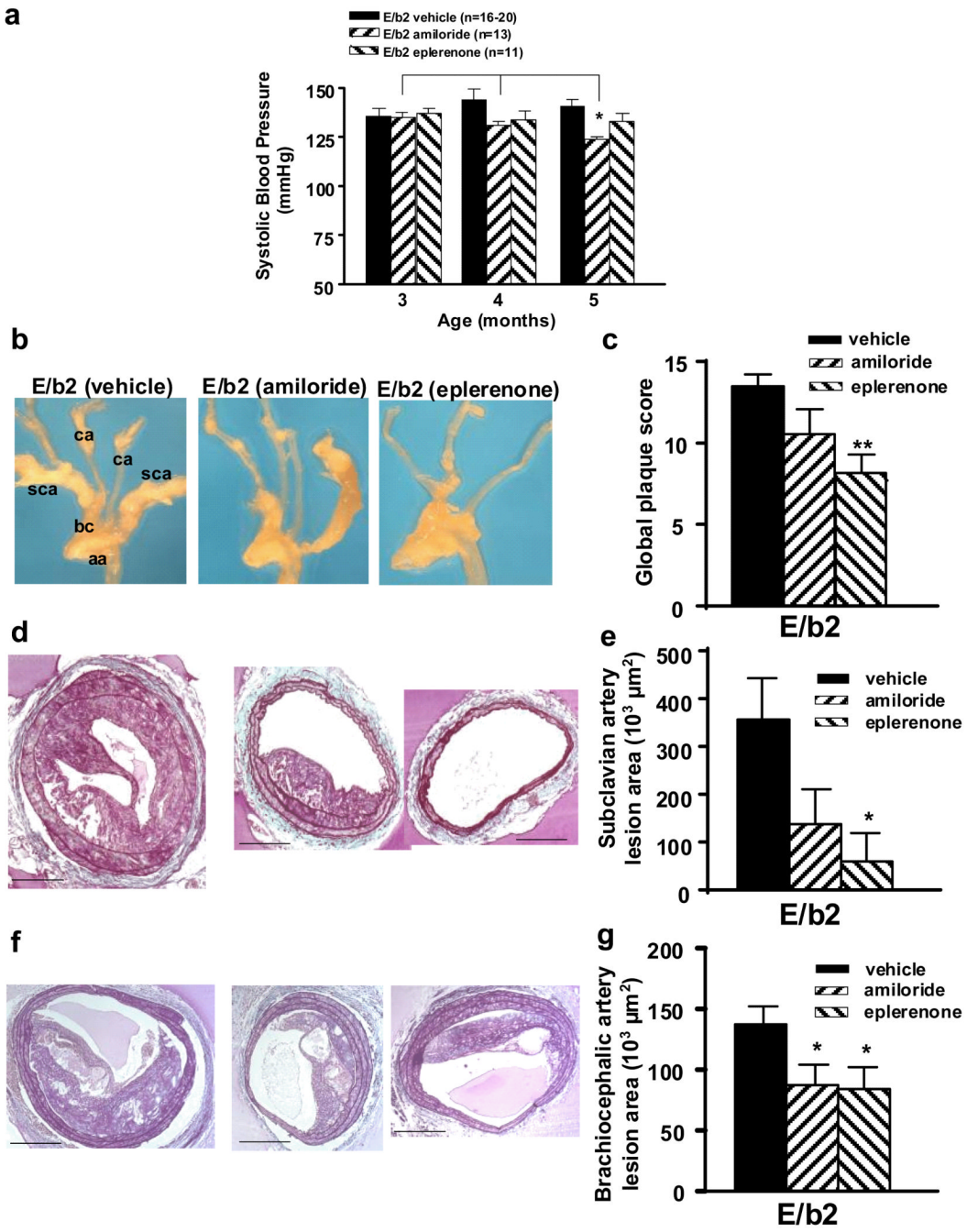

Figure 4. Eplerenone reduces lesion size in E/b2 mice, independently of blood pressure

(a) Systolic blood pressure in E/b2 and *Apoe*$^{-/-}$ mice was reduced in E/b2 mice by treatment with amiloride but not by eplerenone. *, $P<0.05$ versus age 3 and 4 months, repeated measures ANOVA

(b) Representative images of the aortic arch and its branches in 5 month-old E/b2 mice after vehicle (left panel), amiloride (centre panel) or eplerenone (right panel) treatment; aa, aortic arch; ca, carotid artery; sca, subclavian artery; bc, brachiocephalic artery.

(c) semi-quantitative analysis of lesion development using global plaque score (see Methods for details). **, $P<0.01$ vs untreated E/b2 Kruskal–Wallis test, n=6–11.

Europe PMC Funders Author Manuscripts
Europe PMC Funders Author Manuscripts

(d) Representative images of US Trichrome-stained plaques in subclavian arteries of 5 month-old E/b2 mice after vehicle (left), amiloride (centre) and eplerenone (right) treatment. Images captured at magnification x10. Scale bar = 250 μm.
(e) Measurement of lesion size; *, $P<0.05$ versus untreated E/b2 mice, 1-way ANOVA, n=4–5).
(f), Representative images of US Trichrome-stained plaques in brachiocephalic arteries of E/b2 mice after vehicle (left), amiloride (centre) and eplerenone (right) treatment. Images captured at magnification x10. Scale bar = 250 μm.
(g) Measurement of lesion size; *, P<0.05 versus untreated E/b2; 2-way ANOVA, n=7-10.

Europe PMC Funders Author Manuscripts
Europe PMC Funders Author Manuscripts

Europe PMC Funders Author Manuscripts

Europe PMC Funders Author Manuscripts

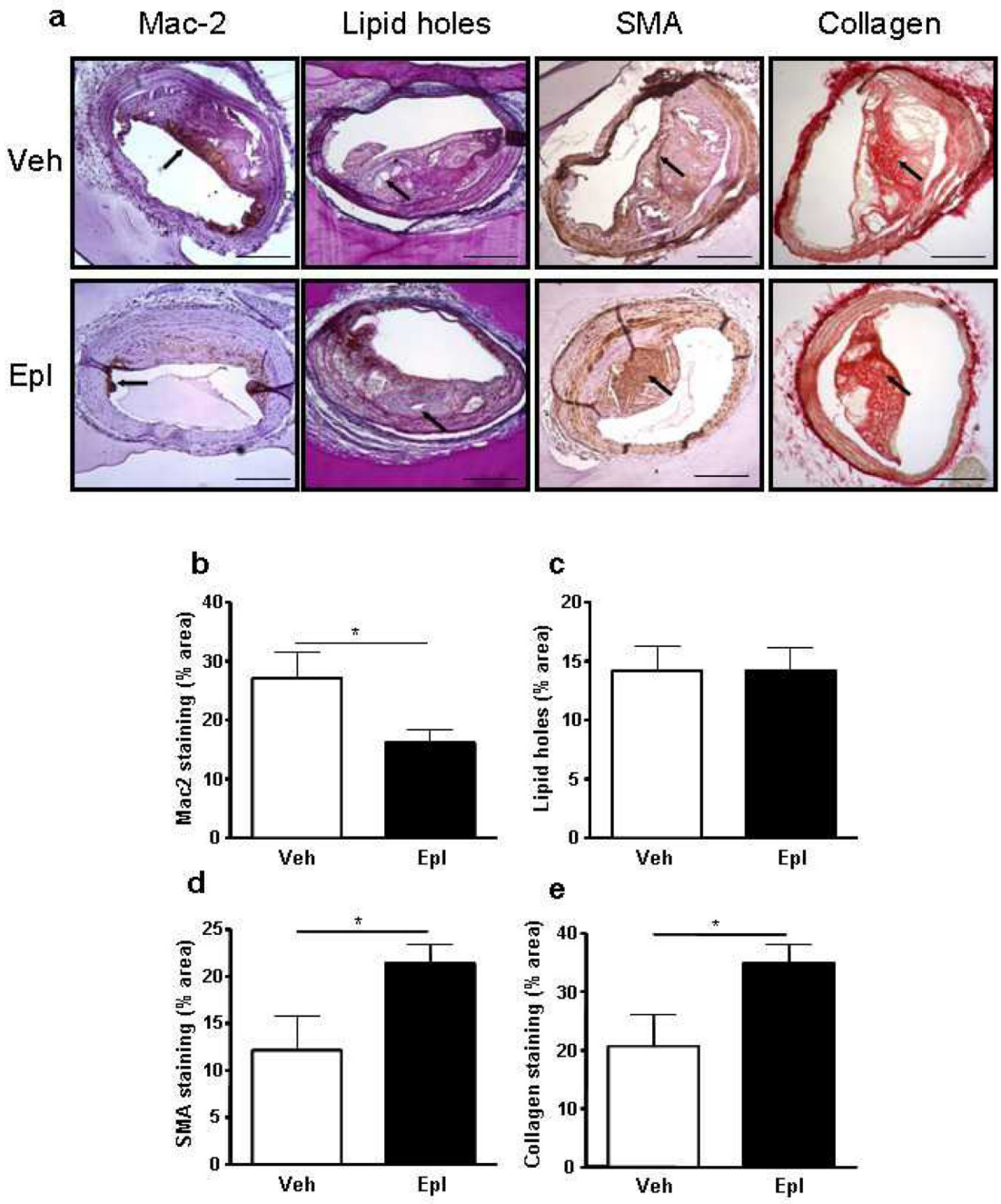

Figure 5. MR blockade reduces macrophage infiltration and alters plaque composition in E/b2 mice

(a) Representative images of atherosclerotic plaques from vehicle- (top panels) and eplerenone-treated (200mg/kg/day; lower panels) E/b2 mice, stained with US Trichrome (lipid holes), Mac-2 antibody (Mac-2), α-SMA antibody (SMA) or Picrosirius red (collagen), captured at x10 magnification. Arrows indicate regions of interest corresponding to names of each column. Scale bar = 250 μm. Compared to vehicle-treated mice, plaques in eplerenone-treated E/b2 mice demonstrated reduced Mac-2 staining (b) with increased staining for α-SMA (d) and collagen (e). There was no apparent difference in lipid content, compared to plaques in vehicle treated E/b2 mice (c). The area of staining was quantified

using Photoshop CS3 Extended software and expressed as a % of total plaque area. Data are mean ± sem, n= 4-5. Analysed by Student's unpaired t test: * $p<0.05$.

Europe PMC Funders Author Manuscripts

Europe PMC Funders Author Manuscripts

Europe PMC Funders Author Manuscripts

Europe PMC Funders Author Manuscripts

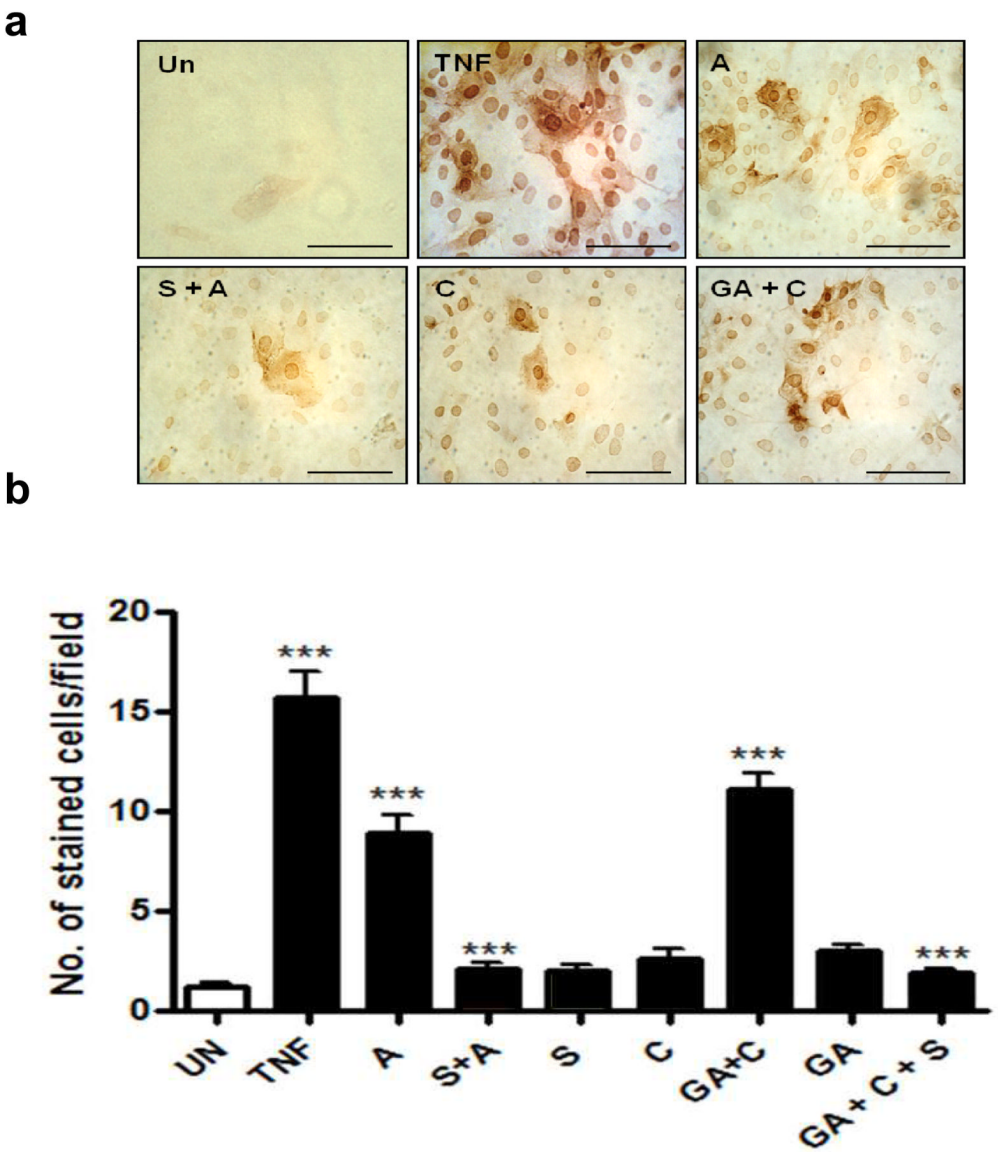

Figure 6. VCAM-1 is induced following mineralocorticoid receptor activation by glucocorticoids in mouse aortic endothelial cells

(a) MAECs were treated for 24h with 10ng/ml TNF-α, 1nM aldosterone (A), or 1nM corticosterone (C), with or without pre-treatment with 1μM spironolactone (S) or 1μM glycyrrhetinic acid (GA) for 2h prior to addition of aldosterone or corticosterone, as indicated. Un = untreated cells. Brown staining shows VCAM-1 immunoreactivity. Images captured at x40 magnification. Scale bar = 250 μm.

(b) VCAM-1 immunopositive cells were counted in 4 randomly selected fields (x40 magnification) per treatment in 5 separate experiments. Data are mean ± sem of 5 experiments. Data were analysed by one-way ANOVA; *** $p<0.0001$.

Europe PMC Funders Author Manuscripts

Europe PMC Funders Author Manuscripts

Table 1

Increased atherogenesis in *ApoE*$^{-/-}$/*Hsd11b2*$^{-/-}$ (E/b2) mice.

	3 months		6 months	
	***Apoe*$^{-/-}$ (4)**	**E/b2 (8)**	***Apoe*$^{-/-}$ (6)**	**E/b2 (8)**
Area inside EEL (x 10^3 μm^2)	100 ± 18	243 ± 30*	182 ± 24	352 ± 27**
Medial Area (x 10^3 μm^2)	39.6 ± 9.1	100.2 ± 10.4**	53 ± 7.3	110 ± 5.4**
Lesion Area (x 10^3 μm^2)	1.4 ± 1.4	48.1 ± 13.9*	8.3 ± 7.1	151.0 ± 15.8**
Lumen Area (x 10^3 μm^2)	59.0 ± 10.0	95.0 ± 12.0	127 ± 15.2	90.0 ± 16
Buried Caps	0	0	0	1.86 ± 0.24**
Macrophages % plaque area	0 (no plaques)	13.9 ± 5.2 (4)	7.7 ± 2.4 (4)	22.5 ± 2.1** (5)

Histological analysis of brachiocephalic arteries identified extensive atherosclerotic lesions in E/b2 mice 3 month old but not in age-matched *Apoe*$^{-/-}$ mice. At 6 months of age, lesion size remained significantly increased in E/b2 compared with *Apoe*$^{-/-}$ mice. The differences in lesion size were significant whether expressed as mm^2 or as a percentage of the lesion area (lesion / area inside the external elastic lamina × 100; Figure 1). Increased lesion development in E/b2 mice reduced the percentage luminal area (lumen / lumen + lesion area × 100), compared with *Apoe*$^{-/-}$ mice mice at both 3 and 6 months of age (Figure 1). Absolute lumen area (mm^2) was not reduced in E/b2 mice due to extensive outward remodelling of the vessel (indicated by increased total area within the external elastic lamina). Buried fibrous caps were evident only in 6 month old E/b2 mice. These may be an indication of lesion 'vulnerability'. Date are mean+s.e.mean, with group sizes shown in parentheses (n).

* $P<0.05$ and

** $P<0.01$ compared to age-matched *Apoe*$^{-/-}$ mice (Student's unpaired t-test). EEL, external elastic lamina.

Europe PMC Funders Author Manuscripts

Europe PMC Funders Author Manuscripts

Table 2

Histological analysis of the effect of treatment with amiloride or eplerenone on atherosclerotic lesion development in the brachiocephalic artery of E/b2 mice and *Apoe*$^{-/-}$ mice.

	E/b2			*Apoe*$^{-/-}$
	Vehicle (10)	**Amiloride (7)**	**Eplerenone (9)**	**Vehicle (10)**
Area inside EEL (x10^3 μm^2)	400 ± 25.0***	321 ± 27.2*	304 ± 33.8**	177 ± 9
Medial Area (x10^3 μm^2)	119 ± 8.6***	96.8 ± 5.0	89.6 ± 8.7**	51.4 ± 3.7
Lesion Area (x10^3 μm^2)	137 ± 15.4***	87.2 ± 17.2*	83.9 ± 19.1**	5.8 ± 3.9
Lumen Area (x10^3 μm^2)	144.4 ± 9.7	137.6 ± 19.8	130.5 ± 10.4	119.7 ± 6.7
Buried Caps	1.1 ± 0.31	0.86 ± 0.26	0.56 ± 0.18	0

Vehicle-treated E/b2 mice demonstrated significant remodeling and atherosclerotic lesion formation compared to vehicle treated *Apoe*$^{-/-}$ mice;

*** $P<0.001$; genotype comparison by Student's unpaired t-test.

Treatment of E/b2 mice with either amiloride or eplerenone significantly reduced the degree of vascular remodeling and atherosclerotic lesion formation in this vascular bed;

* $P<0.05$;

** $P<0.01$ when compared with vehicle treated E/b2 mice, 2-way ANOVA.